ChemPubSoc Europe

DOI: 10.1002/chem.201905479

CHEMISTRY A European Journal Full Paper

Ruthenium Catalysis |*Hot Paper*|

# In Situ Structural Determination of a Homogeneous Ruthenium Racemization Catalyst and Its Activated Intermediates Using X-Ray Absorption Spectroscopy

Karl P. J. Gustafson[+],[a, b, d] Arnar Guðmundsson[+],[a] Éva G. Bajnóczi[+],[c, e] Ning Yuan,[b, c] Xiaodong Zou,*[b] Ingmar Persson,*[c] and Jan-E. Bäckvall*[a]

**Abstract:** The activation process of a known Ru-catalyst, dicarbonyl(pentaphenylcyclopentadienyl)ruthenium chloride, has been studied in detail using time resolved in situ X-ray absorption spectroscopy. The data provide bond lengths of the species involved in the process as well as information about bond formation and bond breaking. On addition of potassium *tert*-butoxide, the catalyst is activated and an alkoxide complex is formed. The catalyst activation proceeds via a key acyl intermediate, which gives rise to a complete structural change in the coordination environment around the Ru atom. The rate of activation for the different catalysts was found to be highly dependent on the electronic properties of the cyclopentadienyl ligand. During catalytic racemization of 1-phenylethanol a fast-dynamic equilibrium was observed.

## Introduction

Knowledge about catalyst activation is crucial for the development of new catalysts and catalytic processes. When studying the activation mechanism of a transition metal complex one is often limited to indirect methods. Reaction intermediates are generally transient, but in some cases, it is possible to accumulate them for characterization by manipulating the reaction parameters. However, it is rarely possible to obtain specific bond lengths of transient metal intermediates using methods such as single-crystal X-ray diffraction.

X-ray absorption spectroscopy (XAS) is an element-specific technique used to determine the local structure around an absorbing element.[1] Unlike single-crystal X-ray diffraction, XAS can be applied to systems in all forms of aggregation and requires only an elemental concentration in the millimolar range. In situ/operando XAS has predominantly been applied to heterogeneous catalysts, and only limited examples of homogeneous metal catalysts have been reported.[2–7] The group of Berry utilized XAS in combination with other spectroscopic techniques to strengthen the „push–pull" mechanism in the bi-rhodium-catalysed carbene and nitrene transfer reactions, and this mechanism was later confirmed by the group of Fürstner.[8,9] In seminal work by the group of Lei on copper-mediated cross-couplings, XAS was used to show that $Cu^{I}$ species were the catalytically active intermediates in the mixture, whereas $Cu^{II}$- and $Cu^{0}$-species acted as spectators.[10,11] XAS has also been applied to other elements in attempts to elucidate catalytic species.[5,12–16] In the few reports that exist, to the best of our knowledge, the emphasis lies either on the X-ray absorption near edge structure (XANES) in an operando setup[17] or on accumulated intermediates.[18,19] Alternatively, studies are performed on very simple systems with high symmetry or under conditions that do not provide time-resolved structural information of enough quality. Herein, we report an in situ XAS that allows for the structural determination of a transient metal intermediate in a ruthenium-catalysed reaction.

[a] *Dr. K. P. J. Gustafson,[+] A. Guðmundsson,[+] Prof. J.-E. Bäckvall*
*Department of Organic Chemistry, Arrhenius Laboratory*
*Stockholm University, 10691 Stockholm (Sweden)*
*E-mail: jeb@organ.su.se*

[b] *Dr. K. P. J. Gustafson,[+] Dr. N. Yuan, Prof. X. Zou*
*Department of Materials and Environmental Chemistry*
*Arrhenius Laboratory*
*Stockholm University, 10691 Stockholm (Sweden)*
*E-mail: xzou@mmk.su.se*

[c] *Dr. É. G. Bajnóczi,[+] Dr. N. Yuan, Prof. I. Persson*
*Department of Molecular Sciences*
*Swedish University of Agricultural Sciences*
*P.O. Box 7015, 75007 Uppsala (Sweden)*
*E-mail: ingmar.persson@slu.se*

[d] *Dr. K. P. J. Gustafson[+]*
*Present address: Borregaard, P.O. Box 162*
*1701 Sarpsborg (Norway)*

[e] *Dr. É. G. Bajnóczi[+]*
*Present address: Wigner Research Centre for Physics*
*Konkoly-Thege Miklós út 29–33*
*1121 Budapest (Hungary)*

[+] *Karl P. J. Gustafson, Arnar Guðmundsson and Éva G. Bajnóczi contributed equally to this work.*

*Supporting information and the ORCID identification number(s) for the author(s) of this article can be found under: https://doi.org/10.1002/chem.201905479.*

Metal-carbonyls are very common in modern coordination and organometallic chemistry, and they are frequently found as reagents or catalysts in organic synthesis.[20] Dicarbonyl(pentaphenylcyclopentadienyl)ruthenium chloride (**1 a**) is formally a transfer hydrogenation catalyst, which has found numerous applications as racemization catalyst in dynamic kinetic resolution (DKR) of a wide range of alcohols.[21–27] The mechanism for the hydride transfer of alcohols with catalyst **1** and related complexes has long been a topic of discussion and dispute.[28–37] The current proposed mechanism starts with activation of the Ru chloride complex **1** by potassium *tert*-butoxide, to give *tert*-butoxide complex **3** (Scheme 1).[21,33,38] Upon the addition of a *sec*-alcohol, an alcohol–alkoxide exchange takes place and a new alkoxide complex **4** is formed. Since **4** is an 18-electron complex, a vacant site on Ru is required for the subsequent β-hydride elimination step, in which the hydride is abstracted from the alkoxide. This vacant site was proposed to be generated through a CO dissociation on the basis of DFT calculations,[32] and this pathway was later confirmed by $^{13}CO$ exchange studies.[39] The CO dissociation enables the subsequent β-hydride elimination to occur, which gives complex *Int*-**1** (Scheme 1). Hydride re-addition to the ketone followed by CO coordination would produce the racemic ruthenium alkoxide complex **4**. Release of the alcohol through another alcohol–alkoxide exchange closes the catalytic cycle.

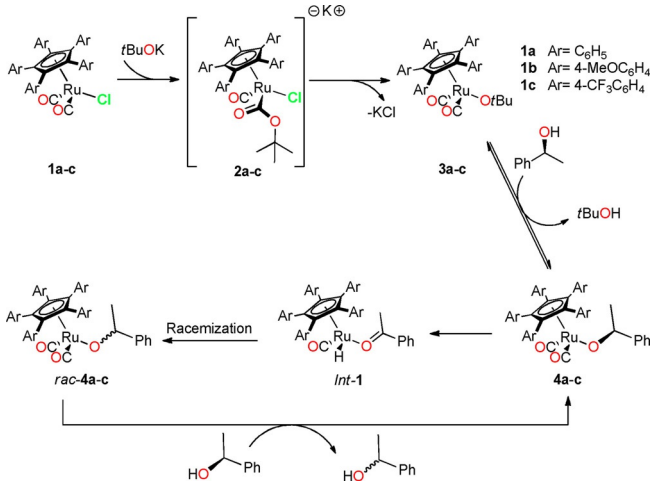


**Scheme 1.** Proposed mechanism of catalyst **1 a** for racemization of *sec*-alcohols.

In an early computational work, catalyst activation and alcohol–alkoxide exchange were proposed to proceed via acyl intermediate **2 a** (Scheme 1).[32] In a subsequent report, experimental evidence for this intermediate acyl complex during activation of the catalyst was provided through the use of in situ FT-IR spectroscopy under cryogenic conditions.[33] Low temperature $^{13}C$ NMR was consistent with the proposed acyl intermediate.[33] An XAS study of catalyst **1 a** and its intermediates would provide important structural information of the environment around the Ru, which has not been possible to obtain before with previous methods.

To reach this goal a temperature and stirring controlled in situ/operando reactor[40] has been applied in the present study. The in situ/operando reactor was recently successfully used to obtain structural information on in-house developed heterogeneous catalysts in operando studies.[41,42]

The aim of the present work has been to study the activation process of $Ru^{II}$ catalysts **1 a–c** utilizing synchrotron radiation in an in situ XAS setup using in situ/operando reactor.

## Results and Discussion

### In situ IR

Activation of catalyst **1 a** as well as the in situ IR studies of acyl intermediate **2 a** have previously only been performed in toluene.[33] Tetrahydrofuran (THF), previously utilized in a DKR study with **1 a**,[43] is a solvent in which the metal complex **1 a–c** has an increased solubility. A higher concentration of the catalysts provides an increased signal to noise ratio, which is required when using the custom-made glass reactor in an in situ/operando XAS setup. Initial studies on monitoring the reaction in THF with in situ IR and $^{13}C$ NMR confirmed that the structural changes follow the same pattern as those reported in toluene[33] (IR spectrum is shown in Figure 1). The main difference between the IR spectra in THF and toluene is that the lifetime of intermediate **2 a** (characteristic peak at 1933 $cm^{-1}$) is significantly prolonged in THF compared to in toluene. In toluene, full conversion to **3 a** took less than 5 min, whereas in THF the same reaction took about 2 h. To confirm that the reaction proceeds through the same mechanism in the two different solvents, and that THF only stabilizes intermediate complex **2 a**, the reaction rate was measured at varying concentrations. From these studies it became clear that the chloride abstraction follows first order kinetics (see Figure S1 and S2). The longer lifetime in THF for anion **2 a** compared to that in tolu-

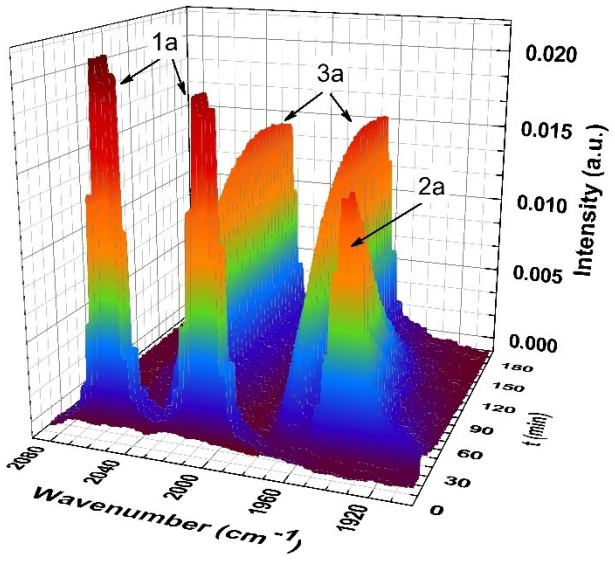


**Figure 1.** Time resolved in situ IR spectrum of the activation of **1 a** by *tert*-BuOK in THF, focused on 2090–1912 $cm^{-1}$ over the time.

 

ene can be explained by the stronger solvation of the charged intermediate by the polar THF compared to the apolar toluene. When adding the substrate, 1-phenylethanol, to the activated complex **3a**, the IR signals of the carbonyls of **3a** slightly blue-shifted immediately and the new complex **4a** formed instantaneously (Figure S3).

In the $^{13}C$ NMR recorded during the activation of catalyst **1a**, the characteristic carbonyl peaks of **2a** were observed in [$D_8$]THF at 209.0 and 208.3 ppm. This observation rules out the possibility that **2a** is a complex formed through simple $Cl^-$ dissociation.

In the FT-IR spectrum of **2a** in toluene[33] the acyl carbonyl peak was observed at 1596 $cm^{-1}$. The $^{13}C$ NMR and the FT-IR of **2a** are not compatible with two equivalent carbon monoxide ligands.

$Cl^-$ dissociation would in principle be possible to detect by Cl K-edge measurements.[44] However, in light of the evidence against $Cl^-$ dissociation (vide infra and supra), and the fact that Cl K-edge EXAFS are not possible to perform to evaluate distances around Cl at the concentrations available in the systems under study as transmission experiments which are required for a correct interpretation,[45] such experiments have not been performed.

## XANES

The XANES spectra of catalyst **1a** in both toluene and THF are identical, confirming that the local structure around Ru is preserved regardless of the applied solvent (see Figure S6). The K-edge was observed at 22125 eV, determined from the first inflection point of the edge using the first derivative of the absorption edge. This observation verifies that the oxidation state of the Ru catalyst is +II. The fact that the edge energy did not change significantly neither during the activation, nor during the catalysis suggests that the oxidation state remained unchanged during the whole process.[46] However, a slight edge shift of 0.6 eV is shown towards lower energies upon the addition of the *t*BuOK, whereas this shift disappears towards reaching the activated state (see Figure S5). This slight edge shift towards lower energies can be explained by the „loss" of one CO ligand (transforms into an acyl group), therefore the decrease of electron back-donation from the ruthenium, leading to a slightly higher electron density around the metal. The XANES spectra of catalysts **1a**, **1b** and **1c** show similar features (see Figure 2 for **1a** and **1b** and Figure S7 for **1c**), suggesting that even though the electronic properties of the substituted cyclopentadienyl (Cp) ligand change from electron-rich to electron-deficient, the aryl groups on the Cp ligand are too far from the $Ru^{II}$ centre to influence its local geometry.

The XANES spectra showed an instantaneous change after the addition of the activator potassium *tert*-butoxide (*t*BuOK). The stronger peak around 22135 eV showed a slight loss in intensity as well as a shift towards higher energy. However, the most noteworthy change in the XANES region is the complete disappearance of the peak around 22160 eV after 5 min (Figure 2a, *cf.* spectrum 1a-0 min and 1a-5 min), which suggests considerable alteration of the environment around Ru. This peak regains its former shape after approximately 45 minutes,

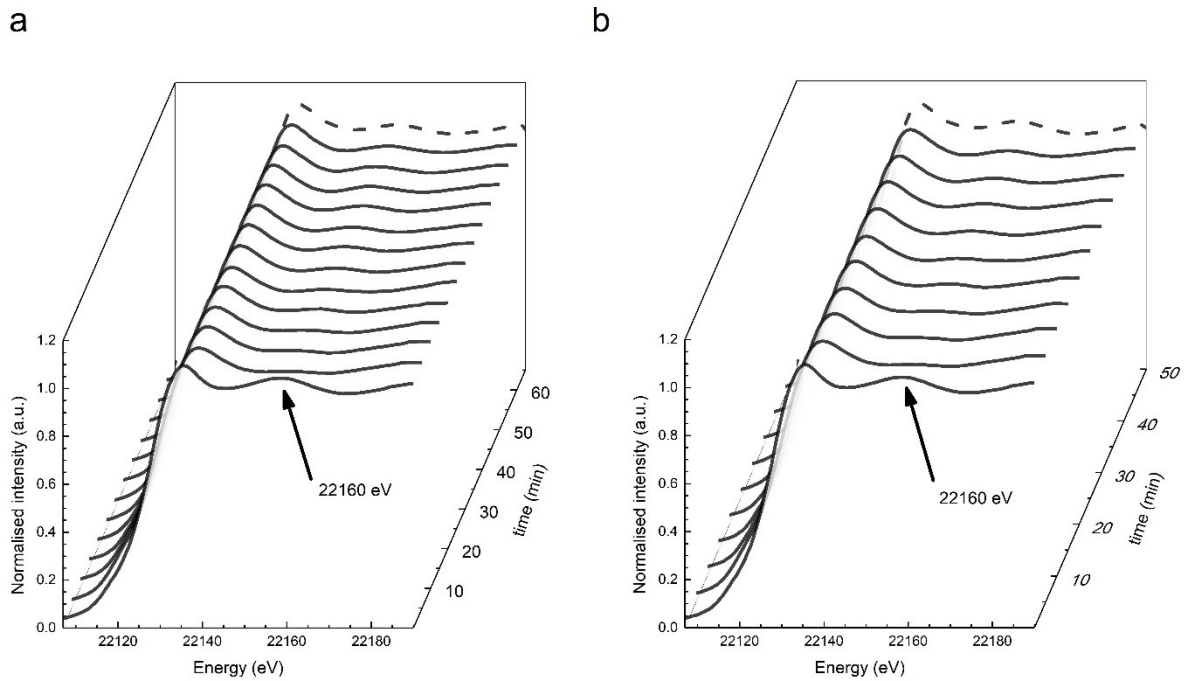


**Figure 2.** a) The normalized XANES spectra of catalyst **1a** dissolved in THF during the activation process recorded every 5 minutes after the addition of *t*BuOK (the measurements were started within 1 min after the addition of *t*BuOK) and after the addition of 1-phenylethanol (added after 65 min) as substrate (dashed line). b) The normalized XANES spectra of catalyst **1b** dissolved in THF, during the activation process recorded every 5 minutes after the addition of *t*BuOK (the measurements were started within 1 min after the addition of *t*BuOK) and after the addition of 1-phenylethanol (added after 50 min) as substrate (dashed line).

after which no further change was observed in the XANES spectrum. The intensity of the peak around 22160 eV never reached that of the original catalyst. After 65 minutes, 1-phenylethanol was added, which led to no significant change of the XANES spectrum (dashed line, Figure 2a), suggesting that the local structure of complex **3a** and **4a** is very similar, but not necessarily identical to that of the initial catalyst **1a**.

The same features in the XANES spectra were observed for catalyst **1b**, although at an increased reaction rate compared to that of **1a**, with no more changes being observed after ≈25 minutes (see Figure 2b). After 50 minutes, 1-phenylethanol was added (dashed line). The results show that the activation process is considerably faster when the aryl groups on the Cp ligand are changed from $C_6H_5$ to the electron-donating 4-MeO-$C_6H_4$, as in the case of **1b**. On the other hand, electron-withdrawing aryl groups on the Cp ligand, as in the case of **1c**, slow down the process significantly.[47] The spectra of catalyst **1c** collected at 5 minutes and after 24 h after starting the activation process are almost identical (see Figure S7). The spectra at 5 minutes are almost identical for all three catalysts, implying that an intermediate state is quickly formed, which is subsequently transformed into the activated catalyst. The rate of the latter step is strongly dependent on the electronic properties of the substituted Cp ligand.

The characteristic features of XANES-spectra, and the increasing intensity of the peak at 22160 eV for catalyst **1a** and **1b** can be used to extract rates and to calculate the approximate half-life for the complexes during activation. Figure 3 shows the normalized intensity values measured at this energy as a function of time. From these curves, the half-life time ($t_{1/2}$) of the intermediates of the activation process was obtained and found to be 28±6 and 6±0.5 minutes for catalysts **1a** and **1b**, respectively. Hence the activation process for **1b** is almost 5 times faster than that of catalyst **1a**. Note that these values are only estimated ones, as other geometrical changes also can have an effect at this energy, but as the activation mechanism is the same in all cases, they play the same role in all measurements, allowing a viable comparison. The reaction with catalyst **1a** monitored by in situ IR shows a similar rate as that observed in the XANES measurements. The slight difference between the two measurements may be due to that the synchrotron irradiation changes the kinetics of the reaction.

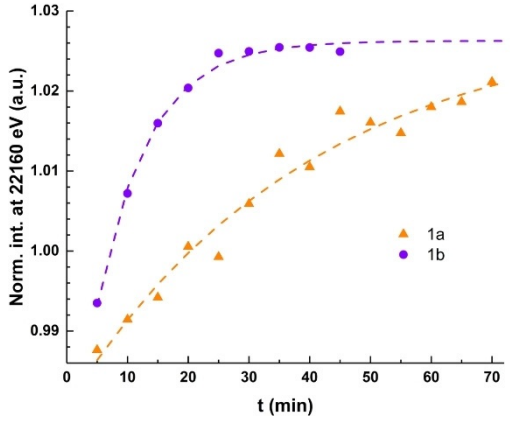


**Figure 3.** Normalized intensity values measured in the XANES at the characteristic peak at 22160 eV as a function of time during the activation process of catalyst **1a** and **1b**.

Complex **1a** dissolved in THF shows only a marginal pre-edge structural change in the XANES spectrum (see Supporting Information, Figure S9a). After addition of the activator, *t*BuOK, the pre-edge feature slightly shifts and becomes more distinct, indicating that the symmetry decreases around the $Ru^{II}$ centre as intermediate **2a** is formed. Interestingly, over time the pre-edge feature decreases again, suggesting that the activated complex **3a** shows a higher symmetry than **2a**. The same trend is seen for catalyst **1b** (see Supporting Information, Figure S9b).

### X-ray absorption fine structure (EXAFS) studies

The coordination environment of ruthenium during the course of the activation was further elucidated by analysing the EXAFS spectra. The Fourier transformed (FT) EXAFS spectra of the dissolved catalyst **1a** in both THF and toluene (see Figure 4 and Figure S10, respectively), show no sign of change compared to those of the solid structure, confirming that the structure of the complex is maintained during the solvation process (Supplementary Information Table S1). When the catalyst is dissolved, its bond lengths are slightly longer than in the solid state. Notably, the distances are a bit longer in THF than in toluene, which is probably due to stronger solvation in THF as it is a more polar solvent. The FT-spectrum of the dissolved catalyst **1a** in THF can be described with two distinct peaks (see Figure 4). The most distinct peak at around 1.8 Å (not phase corrected) corresponds to the interatomic distances of the 2 C atoms of the COs, the 5 C atoms of the Cp ring, and the Cl coordinated to $Ru^{II}$. The refined bond lengths are 1.906, 2.240 and 2.436 Å, respectively (see Table 1). All bond lengths and their corresponding Debye–Waller coefficients are summarized in Table 1. These bond lengths agree well with previously reported single crystal data of complex **1a**.[18] The second distinct peak at approximately 2.5 Å (not phase corrected) corresponds to the Ru···O and Ru-C-O multiple scatterings (MS) of the linear carbon monoxides. These MS events are intensified due to the focusing effect, which plays an important role when two atoms in a coordinating ligand, or part of a larger ligand, form a linear or close to linear M-L-L′ structural motif with the absorbing atom.[48,49] The refined distances for the Ru···O of the carbonyls are 3.045 Å.

The spectra collected during the activation process of catalyst **1a** are given in Figure 4a. The spectra of the catalyst were treated individually, and only representative spectra are presented in Figure 4b, whereas their refined models are presented in Table 1. It is clearly visible in the EXAFS spectra that after only 5 minutes there is an immediate and prominent change in the local structure around $Ru^{II}$ (1a-5 min in Figure 4a and b) as well as an overall loss of intensity. The second main peak, in particular, exhibited a significant drop in intensity, which indicates that the number of coordinating carbon monoxides has decreased. The distinct separation between the two peaks has also disappeared, implying that a new signal has appeared

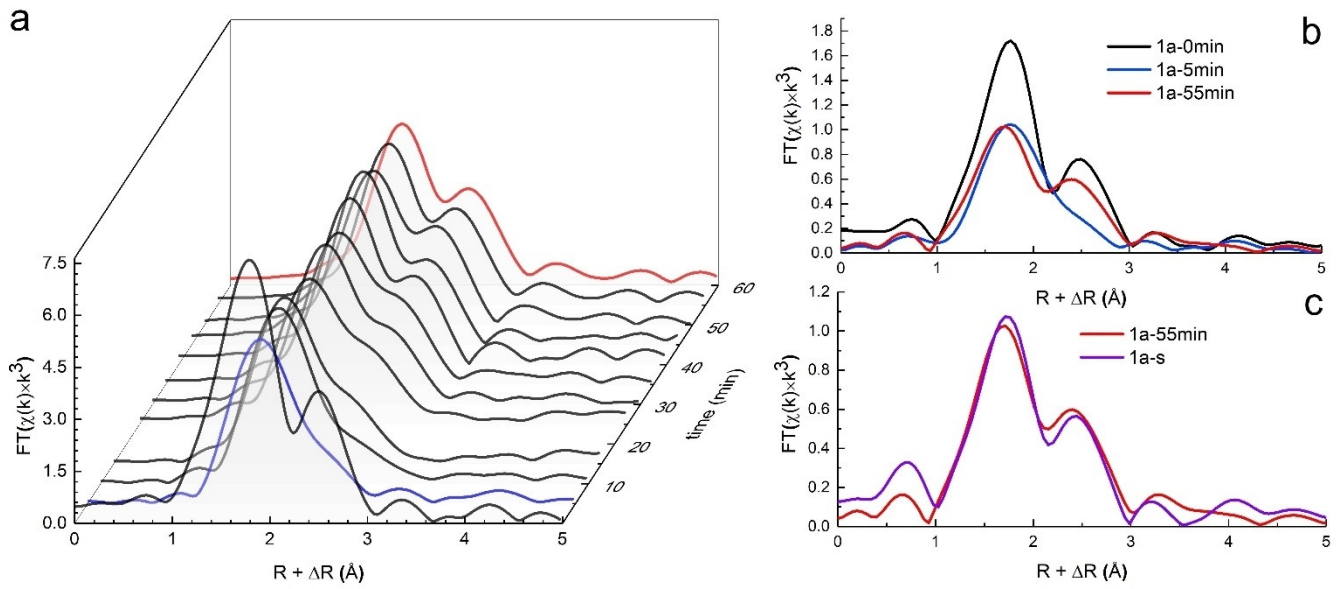


**Figure 4.** a) Fourier transformed EXAFS spectra of catalysts **1 a** over time dissolved in THF (**1 a** in THF), during the course of activation. b) Fourier transform of the EXAFS spectra of catalyst **1 a** dissolved in THF (1a-0 min), and at 5, and 55 minutes after the addition of the *t*BuOK (1a-5 min, and 1a-55 min, respectively). c) Fourier transform of the EXAFS spectra of the activated catalyst **1 a** (1a-55 min) and after the addition of 1-phenylethanol (1a-s). *k*-range 2–10 $Å^{-1}$, no phase correction ($\Delta R \approx 0.5$ Å).

around 2.7 Å. The best fitted model contains five Ru–C distances with an average of 2.269 Å, corresponding to the Cp ring, one Ru–Cl bond with a distance at 2.346 Å, two Ru···O distances of around 2.697 Å and two short Ru–C bond lengths of around 1.859 Å (Table 1). However, the second major peak can be fitted with the MS contribution from only one CO. These distances can be interpreted in such a way that the six coordination sites around $Ru^{II}$ are occupied by the Cp ring (hapticity of 5, three coordination sites on Ru), one Cl, one CO and one acyl ester as in intermediate **2 a**. The Debye–Waller factors are only somewhat larger than the values of **1 a**, which implies that there is one dominant species in the reaction system after 5 minutes with a very minor contribution from a second species.

The shortening of the Ru–Cl bond length from 2.44 to 2.35 Å on going from **1 a** to **2 a** is most likely due to the fact that one CO is reacted into a carboalkoxy group ($CO_2tBu$). With this new ligand the back-donation to Ru is decreased, which leads to a significantly shorter (about 0.08 Å) Ru–Cl bond. A similar shortening affect was observed in the Ru–Cl bond length at a comparison of $(S\text{-dmso})_3Ru^{II}Cl_3^-$, and $O_4RuCl_2$ complexes (see more detailed discussion in the Supporting Information, Tables S4a–c). Furthermore, no complex with the composition RuCl(O-ligand)(CO)(Cp) have been reported indicating the labile character of such complexes.

During the activation process, the most prominent peak centered around 1.8 Å (not phase corrected) moves towards slightly shorter distances. The second main peak, which corresponds to the CO's, increases in intensity and the distinct separation between the two peaks reappears when the activated state **3 a** is reached (1a-55 min in Figure 4 a and b). The main peak has shifted a few tenths of an Ångström towards shorter distances, which suggests that the chloride is lost during the activation. The best fit for the active catalyst corresponds to a coordination environment with the Cp ring, two COs, and the *tert*-BuO bonded to the $Ru^{II}$ (**3 a**), see Table 1 for the refined values.

Catalyst **1 b**, with an electron-donating cyclopentadienyl ring, exhibits the same spectral patterns. Since the reaction of **1 b** is significantly faster than that of **1 a**, the first spectrum collected during the activation (Figure 5, 1b-5 min) is already a mixture of species.

The results of the model fitting strengthen this assumption (Supplementary Information Table S2). To obtain a good fit, the use of a mixture of possible coordinating moieties is necessary, including several factors like broken coordination numbers of the chloride ions, the carbon monoxides, the acyl group and even the *tert*-BuO group. The refined Debye–Waller factors are fairly large, which is consistent with a much faster reaction leading to mixed species. After the reaction had reached the activated complex **3 b** of catalyst **1 b** (Figure 5, 1b-45 min), it can be described with the exact same model as for catalyst **1 a** (Table S2).

It is not possible to distinguish between the two Ru–O distances. The value given is an average of the two Ru–O distances.

During the course of the synchrotron experiments, pre-catalyst **1 c** did not reach the active state **3 c**. It seems that the whole activation process is arrested at the intermediate state **2 c** as shown in Figure 5 b. Even after 24 h there was no significant change in the structure around $Ru^{II}$ (Figure 5 b and Supplementary Information Table S3).

**Table 1.** The *k* space fitted models for the Ru K-edge EXAFS measurement preformed on catalyst **1a** in THF and at different times during the reaction. Number of distances (*N*), mean distances (*R* Å$^{-1}$) and Debye–Waller factor ($\sigma^2$ Å$^{-2}$). The fitted parameters for the multiple scattering paths are omitted for the sake of clarity, and they can be found in Table S1 in the Supporting Information.

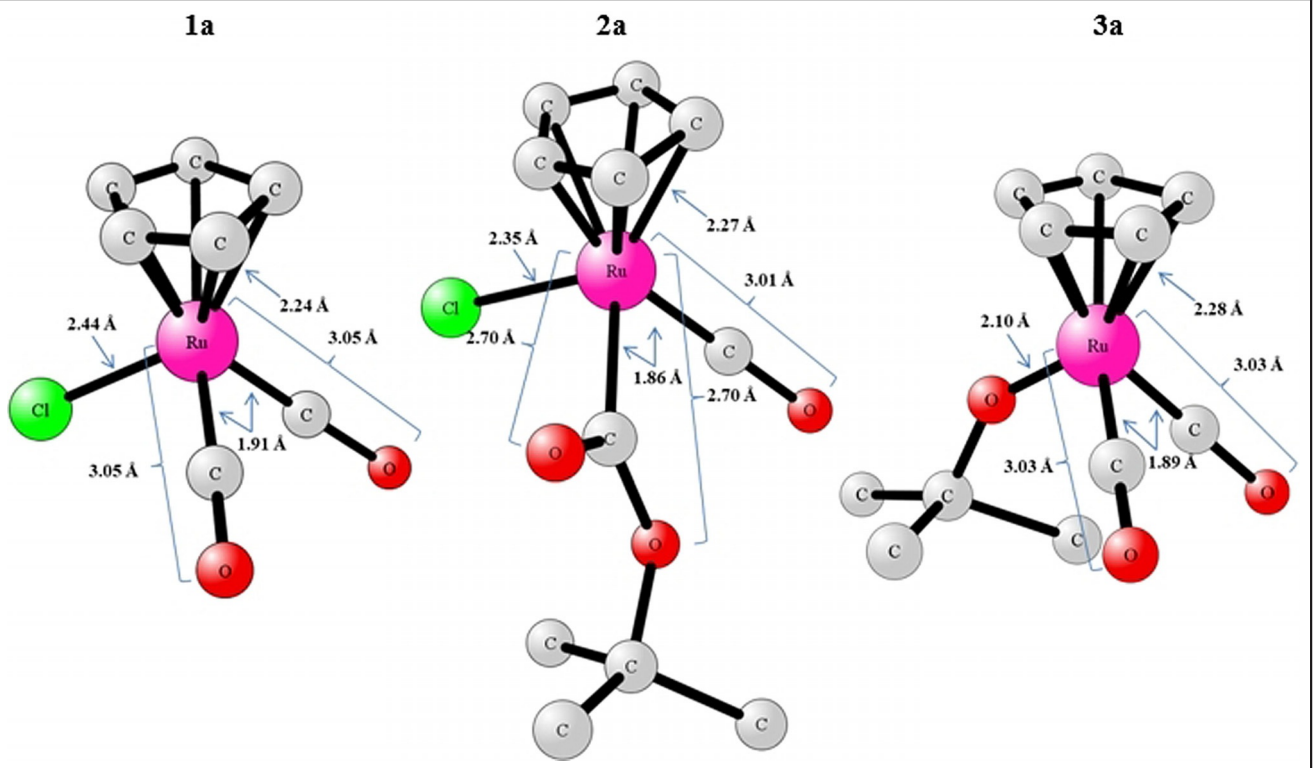


| Structure | Bond | *N* | *R* | $\sigma^2$ |
|---|---|---|---|---|
| 1a-0 min (**1a**) | Ru−**Cp** | 5 | 2.240(8) | 0.0016(9) |
| | Ru−**C**≡O | 2 | 1.906(5) | 0.0018(6) |
| | Ru−C≡**O** | 2 | 3.045(6) | 0.0062(5) |
| | Ru−**Cl** | 1 | 2.436(8) | 0.0044(5) |
| 1a-5 min (**2a**) | Ru−**Cp** | 5 | 2.269(11) | 0.0089(9) |
| | Ru−**C**−O | 2[a] | 1.859(12) | 0.0125(18) |
| | Ru−C≡**O** | 1 | 3.007(18) | 0.0093(9) |
| | Ru−C(=**O**)−**O**-$^t$Bu | 2[b] | 2.697(8) | 0.00361(8) |
| | Ru−**Cl** | 1 | 2.346(6) | 0.0062(9) |
| 1a-55 min (**3a**) | Ru−**Cp** | 5 | 2.278(15) | 0.0039(12) |
| | Ru−**C**≡O | 2 | 1.894(5) | 0.0057(7) |
| | Ru−C≡**O** | 2 | 3.025(12) | 0.0086(4) |
| | Ru−**O**-$^t$Bu | 1 | 2.095(9) | 0.0026(9) |

[a] It is not possible to distinguish between the two Ru–C distances. [b] The value given is an average of the two Ru–C distances.

### Substrate addition

1-Phenylethanol was added to activated complexes **3a** and **3b**, as substrate for the racemization. Following the addition, the XANES spectra of **4a** and **4b** resembled each other (Figure 2, dashed lines), as did their respective Fourier transforms (Figure 4c and inset in Figure 5a). When fitting the refined data, it becomes apparent that the hexa-coordinated structure is maintained in an octahedral configuration around Ru$^{II}$ and the coordination of the Cp ring and the two CO ligands are preserved during catalysis. The last coordination site cannot be identified with certainty. It is most probably a loosely bound oxygen based on the XANES spectrum, although the EXAFS contribution is on the level of noise. The lack of clear identification of the alkoxide ligand in complex **4a–c** suggests that the systems are in dynamic equilibria with fast interconversions of substrate molecules.

## Conclusions

XAS was used to obtain detailed structural information in solution of catalysts **1a–c**, the proposed acyl intermediates **2a–c**, as well as the activated alkoxide complexes **3a** and **3b**. Different rates of activation were observed for the different catalysts, which was highly dependent on the electronic properties of

 

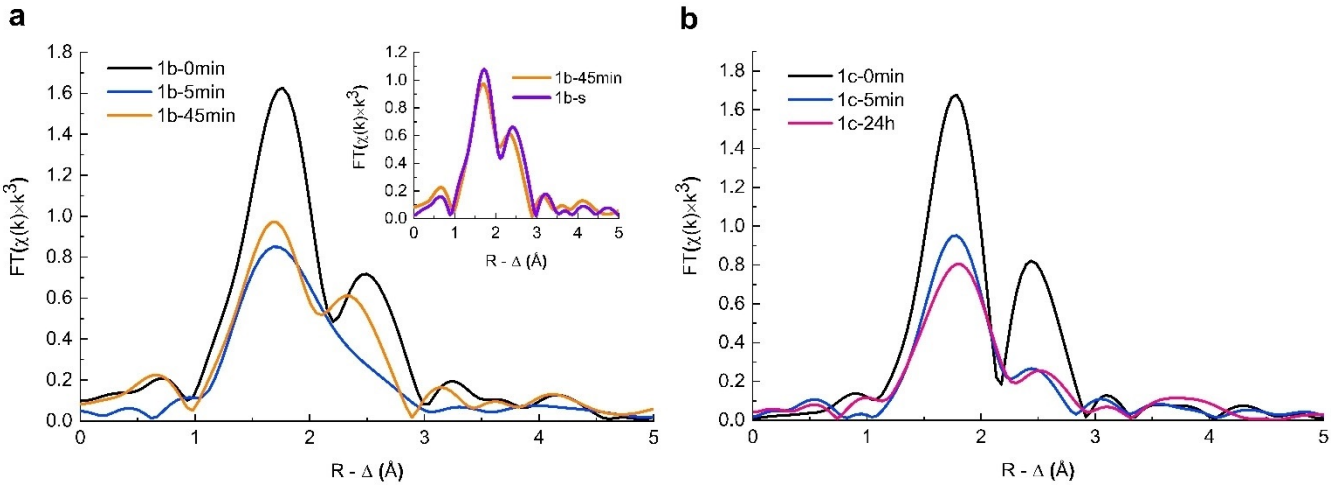


**Figure 5.** a) Fourier transform of the EXAFS spectra of catalyst **1 b** dissolved in THF (1b-0 min), and at 5 and 45 minutes after the addition of *t*BuOK (1b-5 min and 1b-45 min, respectively). The inset shows Fourier transform of the EXAFS spectra of the activated catalyst **1 b** (1a-45 min) and after the addition of 1-phenylethanol (1b–s). k-range 2–10 $Å^{-1}$, no phase correction ($\Delta R \approx 0.5$ Å). b) Fourier transform of the EXAFS spectra of catalyst **1 c** dissolved in THF (1c-0 min), at 5 minutes and 24 hours after the addition of *t*BuOK (1c-5 min and 1c–24 h, respectively), k-range 2–10 $Å^{-1}$, no phase correction ($\Delta R \approx 0.5$ Å).

the Cp ligand. In the case of **1 c**, the strong electron-withdrawing character of the Cp ligand inhibited the activation process. During the catalytic racemization of 1-phenylethanol, a fast-dynamic equilibrium is established between the two enantiomers of **4 a–b** and the ketone *Int*-**1** resulting in less resolved spectra for **4 a** and **4 b**. Therefore, only an average structure was obtained for these compounds.

Information gained from this study may aid in the development of new catalysts and to understand the different modes of activation of different catalysts.

## Experimental Section

### General experimental procedure

$^1$H NMR and $^{13}$C NMR were recorded at 400 MHz and 125 MHz, respectively. Chemical shifts are reported in ppm, using the residual solvent peak in $CDCl_3$ (δH 7.26 or δC 77.16 ) or [$D_8$]THF (δH 3.58 or δC 67.21 ) as internal standard. All solvents were dried prior to use, stored over activated 4 Å molecular sieves under 6.0 argon. Chemicals other than the catalysts were purchased from commercial sources and dried before use. Reactions were monitored using aluminium-packed plates (1.5 Å, 5 cm) which are pre-coated with silica gel (0.25 mm). UV light or $KMnO_4$ was used for visualization. Column chromatography was performed using silica gel (particle size 40–63 μm, mesh size 230–400, pore size 60 Å). Reactions at the synchrotron were performed in a glovebox under argon atmosphere. In situ IR was measured using ReactIR with a zirconium probe in a Schlenk flask which allowed easy connection with the ReactIR probe using a NS 19 fitting and the reactions were performed under 6.0 argon. Ruthenium catalysts **1 a–c** were prepared according to a literature procedure.[47] Caution should be taken when distilling the dicyclopentadiene for the synthesis of the ligand for **1 c**.

### Experimental methods XAS

The Ru K-edge EXAFS measurements of catalyst **1 a** in the solid state and dissolved in toluene were performed at a wiggler-based beam line 4-1 at the Stanford Synchrotron Radiation Lightsource (SSRL), Stanford, USA, operating at 3.0 GeV and 300 mA (top-up mode). The X-rays were monochromatized by a Si[220] double crystal monochromator. The second monochromator crystal was detuned to reflect 75% of the maximum intensity at the end of the scans to minimize the higher order harmonics. All the other ex situ as well as in situ spectra were collected at the undulator based P64 beam line, equipped with a Si[311] double crystal monochromator, at the Petra III Extension, Hamburg, Germany, operating at 6.0 GeV and 100 mA (top-up mode). The energy was internally calibrated in both cases with a metallic Ru foil, with the first inflection point of the K-edge spectrum assigned as 22 117 eV.[50]

For the ex situ measurements, three spectra were collected per sample and they were averaged after energy calibration, while the spectra in the in-situ measurements were treated individually. If not noted differently, the scanning rate was 5 min/scan in the −200–+800 eV energy range around the Ru K-edge. The measurement of the solid was performed in transmission mode, whereas the solution was detected in fluorescence mode using a Lytle detector. The **1 a** catalyst in solid state measured at SSRL was diluted with approximately the same amount of boron nitride (BN, Merck), whereas the toluene solution was contained in a sample made of titanium frame, a Teflon spacer and 6 mm polypropylene X-ray film as windows. The measurements at Petra III were performed in a custom-made temperature-controlled reactor with a glass test tube with 1 mm thick glass walls with the beam hitting as perpendicular as possible. The measurements were performed at ambient room temperature (ca. 25 °C). The reactor is described in detail elsewhere.[40] At Petra III, all spectra were collected in transmission mode using ion-chambers as detectors filled with appropriate gas mixtures. All data treatment (energy calibration, averaging, pre-edge subtraction, spline fitting and removal, normalization and Fourier transformation) were performed with EXAFSPAK program package.[51] The $k^3$-weighted experimental data were fitted by refining the structural parameters using Marquardt non-linear least-square fitting algorithm within the EXAFSPAK package. The following parameters were refined: mean interatomic distance ($R$), Debye–Waller factor coefficients ($\sigma^2$), amplitude reduction factor ($S_0^2$), and the threshold energy ($E_0$). The number of neighbouring atoms were held constant during the fitting process due to strong

correlation between the number of distances and Debye–Waller coefficients. The theoretical phases and amplitudes were calculated with the FEFF7 program.[52]

The standard deviations for the refined parameters were obtained from $k^3$-weighted least-squares refinements of the EXAFS function $\chi(k)$ and did not include systematic errors of the measurements. These statistical error values allowed reasonable comparisons for example, of the significance when comparing relative shifts in distances. However, the variations in the refined parameters, including the shift in the $E_0$ value (for which $k=0$), using different models and data ranges, indicated that the absolute accuracy of the distances given for the separate complexes is within $\pm 0.005$ to 0.02 Å for well-defined interactions. The 'standard deviations' given in the text have been increased accordingly to include estimated additional effects of systematic errors.

### General procedure for in situ XAS

A flame dried vial was placed while hot directly into antechamber of the glovebox and placed under vacuum, then transferred into the glovebox after cooling down. Catalyst **1** (0.10 mmol) was dissolved in 1.8 mL of dry THF and the reaction vial was sealed. XAS spectra were collected on catalyst **1**, the reaction vial was placed back in the glovebox and *t*BuOK (1 M in THF, 100 μL, 0.1 mmol) was added. The reaction vessel was placed back into the beam and the structural changes were monitored over time.

### Experimental procedure for in situ IR measurement of the activation of 1 a

Ruthenium catalyst **1 a** (203 mg, 0.32 mmol) was dissolved in 5 mL of dry THF at room temperature using a flame dried 100 mL Schlenk flask under argon and a series of spectra were recorded (2049 and 2001 $cm^{-1}$) before addition of *t*BuOK (1 M in THF, 320 μL, 0.32 mmol) and the activation was followed in an operando fashion with 15 sec scan interval. Upon addition of the *t*BuOK the solution turned red and the two previous CO signals disappeared, with a new dominant CO signal at 1933 $cm^{-1}$ being observed from complex **2 a**. Gradually over time, the activated complex **3 a** could be observed with the corresponding CO signals at 2021 and 1964 $cm^{-1}$. After the complete disappearance of **2 a**, the substrate, 1-phenylethanol, was added (100 μL, 0.82 mmol) and alkoxide **3 a'** formed instantaneously without an apparent intermediate (CO peaks 2026 and 1971 $cm^{-1}$).

## *Acknowledgements*

Financial support from The Swedish Research Council (2016–03897, 2017–04321), the Berzelii Center EXSELENT, and the Knut and Alice Wallenberg Foundation (CATSS, KAW 2016.0072) is gratefully acknowledged. Parts of this research were carried out at PETRA III at Deutsches Elektronen-Synchrotron (DESY), a member of the Helmholtz Association (HGF). We would like to thank Vadim Murzin and Wolfgang Caliebe for assistance with using the P-64 beamline. Another part of this research was performed at the Stanford Synchrotron Radiation Lightsource, SLAC National Accelerator Laboratory, is supported by the U.S. Department of Energy, Office of Science, Office of Basic Energy Sciences under Contract No. DE-AC02-76SF00515. The SSRL Structural Molecular Biology Program is supported by the DOE Office of Biological and Environmental Research, and by the National Institutes of Health, National Institute of General Medical Sciences (including P41GM103393). The contents of this publication are solely the responsibility of the authors and do not necessarily represent the official views of NIGMS or NIH. We would also like to express our appreciation to Niclas Heidenreich, A. Ken Inge and Sebastian Leubner for their assistance with the reactor.

## Conflict of interest

The authors declare no conflict of interest.

**Keywords:** homogeneous catalysis · in situ EXAFS spectroscopy · racemization · ruthenium

[1] P. Glatzel, U. Bergmann, *Coord. Chem. Rev.* **2005**, *249*, 65 – 95.
[2] S. Bordiga, E. Groppo, G. Agostini, J. A. van Bokhoven, C. Lamberti, *Chem. Rev.* **2013**, *113*, 1736 – 1850.
[3] J. Singh, C. Lamberti, J. A. van Bokhoven, *Chem. Soc. Rev.* **2010**, *39*, 4754.
[4] S. Bordiga, F. Bonino, K. P. Lillerud, C. Lamberti, *Chem. Soc. Rev.* **2010**, *39*, 4885.
[5] S. N. MacMillan, K. M. Lancaster, *ACS Catal.* **2017**, *7*, 1776 – 1791.
[6] G. J. Sherborne, B. N. Nguyen, *Chem. Cent. J.* **2015**, *9*, 37.
[7] D. Koziej, S. DeBeer, *Chem. Mater.* **2017**, *29*, 7051 – 7053.
[8] K. P. Kornecki, J. F. Briones, V. Boyarskikh, F. Fullilove, J. Autschbach, K. E. Schrote, K. M. Lancaster, H. M. L. Davies, J. F. Berry, *Science* **2013**, *342*, 351 – 354.
[9] C. Werlé, R. Goddard, A. Fürstner, *Angew. Chem. Int. Ed.* **2015**, *54*, 15452 – 15456; *Angew. Chem.* **2015**, *127*, 15672 – 15676.
[10] Q. Lu, J. Zhang, P. Peng, G. Zhang, Z. Huang, H. Yi, J. T. Miller, A. Lei, *Chem. Sci.* **2015**, *6*, 4851 – 4854.
[11] C. He, G. Zhang, J. Ke, H. Zhang, J. T. Miller, A. J. Kropf, A. Lei, *J. Am. Chem. Soc.* **2013**, *135*, 488 – 493.
[12] J. Rabeah, M. Bauer, W. Baumann, A. E. C. McConnell, W. F. Gabrielli, P. B. Webb, D. Selent, A. Brückner, *ACS Catal.* **2013**, *3*, 95 – 102.
[13] A. S. K. Hashmi, C. Lothschütz, M. Ackermann, R. Doepp, S. Anantharaman, B. Marchetti, H. Bertagnolli, F. Rominger, *Chem. Eur. J.* **2010**, *16*, 8012 – 8019.
[14] H. Asakura, T. Shishido, T. Tanaka, *J. Phys. Chem. A* **2012**, *116*, 4029 – 4034.
[15] A. R. Corcos, O. Villanueva, R. C. Walroth, S. K. Sharma, J. Bacsa, K. M. Lancaster, C. E. MacBeth, J. F. Berry, *J. Am. Chem. Soc.* **2016**, *138*, 1796 – 1799.
[16] S. K. Sharma, P. S. May, M. B. Jones, S. Lense, K. I. Hardcastle, C. E. MacBeth, *Chem. Commun.* **2011**, *47*, 1827 – 1829.
[17] D. Lebedev, Y. Pineda-Galvan, Y. Tokimaru, A. Fedorov, N. Kaeffer, C. Copéret, Y. Pushkar, *J. Am. Chem. Soc.* **2018**, *140*, 451 – 458.
[18] D. Moonshiram, J. W. Jurss, J. J. Concepcion, T. Zakharova, I. Alperovich, T. J. Meyer, Y. Pushkar, *J. Am. Chem. Soc.* **2012**, *134*, 4625 – 4636.
[19] Y. Pushkar, D. Moonshiram, V. Purohit, L. Yan, I. Alperovich, *J. Am. Chem. Soc.* **2014**, *136*, 11938 – 11945.
[20] M. Zhou, L. Andrews, C. W. Bauschlicher, *Chem. Rev.* **2001**, *101*, 1931 – 1962.
[21] B. Martín-Matute, M. Edin, K. Bogár, J.-E. Bäckvall, *Angew. Chem. Int. Ed.* **2004**, *43*, 6535 – 6539; *Angew. Chem.* **2004**, *116*, 6697 – 6701.
[22] B. Martín-Matute, M. Edin, K. Bogár, F. B. Kaynak, J.-E. Bäckvall, *J. Am. Chem. Soc.* **2005**, *127*, 8817 – 8825.
[23] R. Lihammar, R. Millet, J.-E. Bäckvall, *Adv. Synth. Catal.* **2011**, *353*, 2321 – 2327.
[24] R. Lihammar, R. Millet, J.-E. Bäckvall, *J. Org. Chem.* **2013**, *78*, 12114 – 12120.
[25] R. Lihammar, J. Rönnols, G. Widmalm, J.-E. Bäckvall, *Chem. Eur. J. Chem. Eur.* **2014**, *20*, 14756 – 14762.
[26] A. Träff, R. Lihammar, J.-E. Bäckvall, *J. Org. Chem.* **2011**, *76*, 3917 – 3921.

 

[27] S. Y. Lee, J. M. Murphy, A. Ukai, G. C. Fu, *J. Am. Chem. Soc.* **2012**, *134*, 15149 – 15153.
[28] C. P. Casey, S. W. Singer, D. R. Powell, R. K. Hayashi, M. Kavana, *J. Am. Chem. Soc.* **2001**, *123*, 1090 – 1100.
[29] J. S. M. Samec, A. H. Éll, J. B. Åberg, T. Privalov, L. Eriksson, J.-E. Bäckvall, *J. Am. Chem. Soc.* **2006**, *128*, 14293 – 14305.
[30] C. P. Casey, T. B. Clark, I. A. Guzei, *J. Am. Chem. Soc.* **2007**, *129*, 11821 – 11827.
[31] B. Stewart, J. Nyhlen, B. Martín-Matute, J.-E. Bäckvall, T. Privalov, *Dalton Trans.* **2013**, *42*, 927 – 934.
[32] J. Nyhlén, T. Privalov, J.-E. Bäckvall, *Chem. Eur. J.* **2009**, *15*, 5220 – 5229.
[33] J. B. Åberg, J. Nyhlén, B. Martín-Matute, T. Privalov, J.-E. Bäckvall, *J. Am. Chem. Soc.* **2009**, *131*, 6035.
[34] M. C. Warner, O. Verho, J. E. Bäckvall, *J. Am. Chem. Soc.* **2011**, *133*, 2820 – 2823.
[35] G. A. I. Moustafa, Y. Oki, S. Akai, *Angew. Chem. Int. Ed.* **2018**, *57*, 10278 – 10282; *Angew. Chem.* **2018**, *130*, 10435 – 10439.
[36] D. G. Gusev, D. M. Spasyuk, *ACS Catal.* **2018**, *8*, 6851 – 6861.
[37] B. L. Conley, M. K. Pennington-Boggio, E. Boz, T. J. Williams, *Chem. Rev.* **2010**, *110*, 2294 – 2312.
[38] B. Martín-Matute, J. B. Åberg, M. Edin, J.-E. Bäckvall, *Chem. Eur. J.* **2007**, *13*, 6063 – 6072.
[39] Ref. [34].
[40] N. Heidenreich, U. Rütt, M. Köppen, A. K. Inge, S. Beier, A.-C. Dippel, R. Suren, N. Stock, *Rev. Sci. Instrum.* **2017**, *88*, 104102.
[41] A. Bruneau, K. P. J. Gustafson, N. Yuan, C.-W. Tai, I. Persson, X. Zou, J.-E. Bäckvall, *Chem. Eur. J.* **2017**, *23*, 12886 – 12891.
[42] N. Yuan, V. Pascanu, Z. Huang, A. Valiente, N. Heidenreich, S. Leubner, A. K. Inge, J. Gaar, N. Stock, I. Persson, B. Martín-Matute, X. Zou, *J. Am. Chem. Soc.* **2018**, *140*, 8206 – 8217.
[43] L. Borén, B. Martín-Matute, Y. Xu, A. Córdova, J.-E. Bäckvall, *Chem. Eur. J.* **2006**, *12*, 225 – 232.
[44] L. Yan, R. Zong, Y. Pushkar, *J. Catal.* **2015**, *330*, 255 – 260.
[45] I. Persson, M. Trublet, W. Klysubun, *J. Phys. Chem. A* **2018**, *122*, 7413 – 7420.
[46] K. Mori, M. Kawashima, K. Kagohara, H. Yamashita, *J. Phys. Chem. C* **2008**, *112*, 19449 – 19455.
[47] O. Verho, E. V. Johnston, E. Karlsson, J.-E. Bäckvall, *Chem. Eur. J.* **2011**, *17*, 11216 – 11222.
[48] P. A. Lee, J. B. Pendry, *Phys. Rev. B* **1975**, *11*, 2795 – 2811.
[49] C. A. Ashley, S. Doniach, *Phys. Rev. B* **1975**, *11*, 1279 – 1288.
[50] A. C. Thompson, J. Kirz, D. T. Attwood, E. M. Gullikson, M. R. Howells, J. B. Kortright, Y. Liu, A. L. Robinson, H. Underwood, James, G. P. Williams, et al., *Xdb-New.Pdf*, Berkeley, California, **2009**.
[51] G. N. George, I. J. Pickering,—a suite of computer programs for analysis of X-ray absorption spectra. Stanford Synchrotron Radiation Laboratory, Stanford, Ca, USA, **2000**.
[52] S. I. Zabinsky, J. J. Rehr, A. Ankudinov, R. C. Albers, M. J. Eller, *Phys. Rev. B* **1995**, *52*, 2995 – 3009.

Manuscript received: December 4, 2019
Accepted manuscript online: January 24, 2020
Version of record online: February 25, 2020

 